ICAS Paper No. 70-07

RESEARCH IN HYPERSONIC WAKES

by
Andre Lemay
Director, Aerophysics Division
Defence Research Establishment
Valcartier, Canada

The Seventh Congress of the International Council of the Aeronautical Sciences

CONSIGLIO NAZIONALE DELLE RICERCHE, ROMA, ITALY / SEPTEMBER 14-18, 1970

Price: 400 Lire

RESEARCH ON HYPERSONIC WAKES

A. Lemay
Director Aerophysics Division

Defence Research Establishment Valcartier, Quebec, Canada.

ABSTRACT

Since 1965, significant progress has been achieved in the field of spatially-resolved or point measurements of various aerothermochemical parameters in the turbulent wakes of hypersonic projectiles launched in the ballistic range facilities of DREV. The sequential spark technique for velocity measurements, the electron beam fluorescence probe for mass density determination, the cooled film anemometer for temperature measurements, as well as electrostatic probe techniques have all contributed to the establishment of a growing body of experimental data on fundamental aerothermochemical wake variables.

I. INTRODUCTION

In 1965 the Defence Research Establishment Valcartier (DREV), in collaboration with the Advanced Research Projects Agency (ARPA) undertook to establish the feasibility of making point (i.e. spatially-resolved) measurements in the wakes of hypersonic projectiles in free-flight in ballistic ranges. Previously, DREV had pioneered[1,2] in the development of light gas gun facilities for launching projectiles at hypersonic speeds and its 4 inch diameter projectile launchers were among the largest in the western world [3]. Microwave techniques for the study of hypersonic projectile flow fields had also had their beginning at DREV[4] and the Establishment was an early contributor of data concerning the associated optical radiation [5].

The standard microwave cavity[6] or interferometer measurements [7] of electron density, as well as the schlieren measurements [8,9] of wake growth are examples of time-resolved but spatially-integrated measurements. The requirement for spatially-resolved measurements, particularly in the case of turbulent wakes of reentry bodies, arises from the following considerations. Radar returns from a reentry wake depend on the lengths of the electron trail and the characteristics of the electron density fluctuations in the trail [10,11]; these in turn depend on the electron chemistry of the wake and the turbulent mixing processes in which cooler fluid from outside the wake core is entrained and mixed with the hot gases in the turbulent core. Schlieren wake growth data does not provide a sensitive arbitrator between various turbulent mixing models [12,13]. Integrated electron density measurements, would not, by themselves, provide the means of defining the proper wake chemistry scheme even if the mixing model were known, because of the dependence of the chemistry on the temperature which itself both controls and is controlled by the chemistry [13]. Thus the consensus developed that a program of point measurements was required on the fundamental aerothermochemical variables of the wake, such as velocity, mass density, temperature, electron density, and certain species concentration, with the objective of providing basic experimental data against which a theoretical modeling of the wake could be compared [13].

As originally conceived the DREV-ARPA program was built around 4 or 5 fundamental experiments. The sequential spark was chosen as the tool for measuring wake velocity. The electron beam fluorescence probe appeared excellent for measurement of mass density. Despite their well-known problems regarding interpretation, the electrostatic-type probes seemed perhaps the only possibility of measuring spatially-resolved charge densities. Consideration was given to the mass spectrometer as a possible tool for measuring species concentration. Finally, cooled-film anemometry techniques appeared to offer the means of obtaining mean and fluctuating temperature data in the wake.

With the exception of the mass spectrometer experiment, most of the experimental techniques have either produced significant data or are on threshold of producing. (The mass spectrometer was abandoned as being somewhat beyond the threshold of the state-of-the-art for the time span of the present program.)

It is the purpose of the present paper to survey the experimental wake measurements program at DREV and to enumerate some of its achievements.

II. HYPERSONIC RANGE FACILITIES

The ballistic range facilities of DREV have been described in some detail elsewhere [14,15] and consequently only the most important characteristics of these will be mentioned.

Foremost of the factors of importance for spatially resolved measurements in the wake is the capability to fly a big model. Physical probes cannot be reduced in size indefinitely, and since statistical measurements demand multiple probes or even arrays of probes in the wake, larger wakes permit greater relative separations and consequently less physical blocking or disturbance of the wake. Large models also provide greater time resolution. For example, with a 2.7 inch diameter sphere firing at 15,000 feet/sec, the normalized wake axial velocity (wake velocity/projectile velocity) drops from 30%

in the very near wake to about 6% in 10 milliseconds. The rapid variation in signal amplitudes as well as the apparent frequency shifts due to wake slowdown necessitate division of experimental signals into short segments if a reasonable degree of signal stationarity is to be preserved for the purposes of statistical analysis. For smaller projectiles, the situation is aggravated, and in practice this means it becomes almost impossible to make meaningful statistical measurements in the interesting near wake region for projectiles less than about one inch in diameter.

The two hypersonic ballistic range facilities at DREV are well suited for the investigation of wake phenomenon. Range 3 is a 6 foot diameter flight chamber with a length of 180 feet. The 1.5 inch diameter launcher, using a constant base pressure cycle, is capable of projecting saboted one inch diameter cones and spheres at velocities from about 4000 feet/second to 18,000 feet/second. This range has been used mainly for sequential spark velocity measurements. The large Range 5 facility has a 10 foot cylindrical chamber with a length of over 400 feet; the largest projectile launched from its 4 inch diameter barrel is a 2.7 inch diameter sphere.

In a point measurements program it is extremely important that adequate techniques be available for positioning the hardware of the various experiments with respect to the predicted flight axis and for positioning the actual flight line with respect to the predicted flight line. At DREV, standard optical techniques are used to align the launchers and equipment. The actual flight trajectory is determined from a series of 30° stereo X-ray shadowgraph stations. Catenary wires and plumb lines are used as references. Shadows of the model and reference lines are recorded on vertical X-ray films, permitting the calculation of the position of the model.

The same X-ray stations are used in the measurement of projectile velocity. Triggers placed just before the X-ray stations trigger the X-rays, the displacement of the center of the projectile shadow from the vertical reference lines are measured on the films. The X-ray pulses themselves are used to trigger time counters.

These systems permit determination of positional accuracies to 0.1 inch and 0.2 degrees in attitude on Range 3 and 0.3 inches and 0.1 degrees on Range 5. The accuracy of velocity determination is to within 100 feet/second on both facilities.

Finally, one more important aspect of ballistic range work must be emphasized, that of the effect of the projectile shock wave system. Some references to the possible deleterious effects upon wake measurements of reflecting shocks arising from the reflection of the projectile shock system at the walls of the range do exist in the literature [17,18,19]. However, apparently because of the lack of sensitivity of spatially-integrated measurements to these effects, the subject of reflected shocks in ballistic ranges has only received scant attention until recently [20,21].

The effects of reflected shocks have been seen in all of the experiments at DREV concerned with point measurements. An exploration of the effects of the reflecting shock system converging on the wake has been carried out by Robertson [21] using schlieren movie techniques. The shock has been found capable of pinching the wake momentarily. Secondly, in the presence of asymmetry of the flight line with respect to the cylindrical range tank, either due to an off-axis firing or the presence of some object in the range, the wake can be physically displaced. For example the walkway in Range 5 (Figure 1) is located about 4 feet from the range center, so that a shock reflecting from the walkway arrives about 1.5 milliseconds before the shock reflecting from the roof of the range. Consequently the wake is driven upwards by the walkway shock and then driven down again by the part of the shock reflecting from the roof. This results not only in a modulation of the probe signals due to variation in the mean level of the variable being observed as the wake moves about, but also in a loss of information as to the position of a measuring probe with respect to the wake axis.

A serious effort was undertaken at DREV to find a means of attenuating the projectile shock system at the walls of the range. Four foot diameter cylinders were installed inside Range 5, and tests were carried out using one inch diameter spherical projectiles, thus simulating the reflected shock system produced on Range 5 by 2.7 inch diameter spheres. Various systems thought capable of attenuating shock systems either by deflection or by absorption were installed in the scaled cylinders. These include deflecting wedge designs, both conical and parabolic in profile, multi-screen diffusing devices, acoustic blanket treatments and anechoic acoustic wedges.

Deflecting wedges proved ineffective. Because one must eliminate the shock effect over a considerable length of range, the included angle at the apex of a deflector is large, and the diffracted shock wave about the apex of a deflecting baffle is still quite strong, and the wave becomes progressively stronger as one moves away from the apex. The multi-screen device showed some promise, but is too cumbersome to seriously consider for range use. Acoustic blankets of fiberglas material proved completely unsuccessful, probably for two related reasons. First of all, at low pressures, the fiberglas materials have a high flow resistance, and thus appear to be stiff and reflective even to normal levels of acoustic energy. In addition, the high velocity field behind a strong shock wave from the projectile might be difficult for the material to cope with even at atmospheric pressure.

Fortunately considerable success was achieved using an attenuation treatment (Figure 2) based on smoothly profiled fiberglas wedges. Figure 3 shows a comparison of the reflecting shock system in a bare control cylinder and in the treated cylinder, using Atlantic Research Corporation high frequency pressure transducers. The shocks have been eliminated in the cylinder

lined with smooth wedges. This result is undoubtedly related to the fact that ordinary reflection of a shock wave from a rigid boundary becomes impossible if the angle of incidence of the wave exceeds a certain value. However, while the smooth wedge treatment has eliminated the reflected shocks, in the process some secondary pressure field appears to have been generated which retains some capability of disturbing the wake. It is not surprising that the energy absorption is inefficient at the reduced pressures employed in the tests (mainly about 1 torr) and operation at higher pressures would tend to increase the efficiency of the treatment for the absorption of any "acoustic" pressure field. In practice, the best results are obtained for symmetrically installed treatments.

The probable benefits of such a shock attenuation treatment are thought to be the following:

1. The disturbance to the wake is much reduced and the loss of radial position information is avoided.

2. The shock waves have been eliminated by the treatment and, with them, their capability of processing of the wake chemistry and temperature distribution.

3. It seems probable that the characteristics of the turbulence will be less likely to be disturbed by a residual acoustic disturbance than by fairly strong shock waves [22].

Full scale shock attenuation treatments based on the smoothly profiled fiberglas acoustic wedge design have been installed in the DREV ranges. Figure 4 shows a treated section of Range 5. A moving carriage covered with wedges on the bottom of the range rolls out of the treated section to permit access to the experiments.

III EXPERIMENTAL TECHNIQUES

Sequential Spark Experiment

The technique of using sequences of sparks for the measurement of flow velocities has been treated by various authors [23,24]. This technique is a quantitative flow visualization experiment which operates on a very simple principle. When an electric spark is produced between a pair of electrodes, a low resistance ionized path is created between the electrodes and appreciable ionization persists for about 0.1 millisecond. Subsequent sparks produced during this time interval will follow the ionized path made by the first spark. When a series of sparks of short duration are made across the wake of the projectile at properly selected time intervals, the ionized path due to the first spark is displaced at the velocity of the gases in the wake and each succeeding spark re-illuminates the ionized path. By open shutter photography of the spark traces, a profile of the displacement of the gas is obtained and the wake velocity can be calculated knowing the time interval between the sparks. Figure 5 shows a typical sequence of sparks obtained in the early days of the wake program at DREV.

The instrumentation designed to produce the sparks generates 0.8 microsecond pulses at 90 kilovolts across the electrodes with a maximum current of 20 amperes in the discharge. These high-voltage pulses are sufficient to obtain with ease the formation of a spark path across gaps of 5 to 7 inches at pressures from 10 to 200 torr. The time interval between the sparks can be adjusted to any value from 3 to 150 microseconds. A typical train of pulses for velocity measurement in the wake consists of a series of four pulses at intervals of 3' microseconds in order to form the spark path, followed by a series of 4 pulses at properly selected time intervals. It was found experimentally that large curvatures of the spark path may reduce the accuracy of the measurement. These large curvatures can be avoided by a proper adjustment of the spark intervals. Satisfactory results are obtained when the wake displacement between two sparks is 10 to 20% of the viscous wake width.

Preliminary measurements have indicated that the sparks do not necessarily pass through the center of the wake along a straight path and therefore, a three-dimensional analysis of the spark path is required. This is achieved by a precision stereo system consisting of two cameras at 60 degrees from the flight axis together with horizontal and vertical reference lines to define the geometry. A film reader reproducing the range geometry is used to perform the three-dimensional analysis of the spark traces. It is necessary first of all to locate accurately the flight path of the projectile with respect to the horizontal reference lines. The plates from the stereo spark cameras are then mounted in the stereo projector reading assembly which is aligned by using the vertical and horizontal reference lines. The co-ordinates of numerous points of each spark in the xz and yz planes are determined by standard photogrammetric techniques. Projections of the sparks in Figure 5 are shown in Figure 6 where the x axis is the direction of flight, the z axis is the vertical direction and the y axis is the horizontal one. From these projections, it is a simple matter to obtain axial and lateral velocity distributions.

Figure 7 shows an example of a sample of 12 radial profiles of velocity collected at 300 body diameters behind one inch diameter spheres at 14500 fps and 40 torr. The wake velocity V_w is normalized to the projectile velocity V_∞ and the radial distance R to the sphere diameter D. Study of a number of these samples measured at various axial distances has shown that the shape of the mean radial profiles is well approximated by Gaussian curves. Accordingly, least mean square fits have been made on each of these samples of a modified Gaussian expression of the form:

$$V_w/V_\infty = (1 - R/aD)\,(V_o/V_\infty)\exp(-R^2/\sigma^2)$$

with R/D negative in the second quadrant in Figure 7. In this expression, V_o/V_∞ is the

normalized axial velocity and σ/D is a parameter related to the velocity radius. The factor $(1 - R/aD)$ has been introduced in the equation to account for the asymmetry of the radial profile due to ion mobility: the electric field applied to re-illuminate the already formed ionized path induces a drift velocity of the ions. Calculations for conditions typical of the wake (P_∞ = 40 torr and temperature of 1000°K) indicate a displacement of the ions of 0.1 cm every time the spark path is re-illuminated. To minimize this effect, only the axial displacement between the first two sparks of each sequence has been used to calculate the velocity. The curve in Figure 7 is the asymmetric curve fitted to the data. The rms deviation of the data points with respect to the asymmetric mean curve is 0.0127 or 14.7% when normalized to the axis velocity. This value is reasonable if one takes account of the fact that it sums up contributions from turbulence intensity, goodness-of-fit, and accuracy of the experimental technique.

The results obtained from the least mean squares fits of the samples of data collected at various axial distances behind spheres at 14500 fps are given in Figure 8. Two different size spheres have been used in order to avoid the troublesome interaction with the wake of the shock system arising from the reflection of the projectile bow and wake shock by the cylindrical range tank [20]. Different pressures were used in order to have the same Reynolds' number (based on sphere diameter) of 0.4×10^6. Full symbols in Figure 8 pertain to data measured behind one inch diameter spheres at 40 torr and open symbols to data obtained behind 0.4 inch spheres at 100 torr. Circles are used to indicate the wake axis velocity V_o/V_∞ and squares to indicate the corresponding values of the profile width σ/D. Power laws with slopes of -1 and 1/3 have been fitted to the wake velocity on the axis and the width of the velocity profile respectively. It can be seen that the velocity decays roughly as $(X/D)^{-1}$ in the region covered by the data. The growth of the velocity core follows the well-established 1/3 growth law of wakes. The radius of the wake observed by the schlieren technique [9] is equal to about 1.25 times the value of σ/D indicated in Figure 8.

In Figure 9, a comparison is made between sphere wake velocities measured in ballistic ranges by four different techniques. Full circles repeat the mean axis velocity data given in Figure 8 at Mach 12.8 and a Reynolds' number of 0.4×10^6. Half full circles represent axis velocities measured on individual profiles with the spark technique (M = 9.8 - 12.4, Re = 0.3×10^6). Full triangles are convection velocities of Heckman [25] obtained from the cross correlation of signals from axial arrays of electrostatic probes at Mach 13.2 and Re = 0.55×10^6. These data collected at radial distances of 1.0 to 1.5 body diameters have been corrected for off-axis by assuming Gaussian radial distributions of velocity and by using the fitted σ/D curve of Figure 8. Full squares represent wake velocities measured by Herrmann, Slattery and Clay [9] and determined from the cross correlation of density fluctuations on sequentially exposed schlieren photographs of the turbulent wake (M = 14.5, Re = 0.2×10^6). Open squares refer to mean wake velocities measured by Fox and Rungaldier [26] using hot wires calibrated in a heated jet and operated at temperature close to that of the wake to emphasize the velocity effect (M = 5.8 and Re = 1.6×10^6). The off-axis effect, more important at the smaller axial distances, has not been corrected in this case because the radial distance is not given. Finally open circles represent the wake axis velocities obtained from radial profiles measured with the spark technique at Mach 3.5 and Reynolds number of 0.1 to 0.5×10^6 [27,28]. Full and half full symbols have been used to represent measurements at high Mach number ($M > 10$) and open symbols for low Mach number ($M < 6$). Hypersonic data measured with the spark and electrostatic probe techniques show excellent agreement. Data obtained with the schlieren technique show appreciably lower velocity. This is due to the fact that the technique measures an average velocity across the wake and is possibly biased to measure the edge velocity because of the wake density distribution. The supersonic data show appreciably lower velocity in the intermediate wake region and coincide with hypersonic data past about 1000 body diameters. Asymptotic -2/3 power law decay is obtained from a distance between 1000 and 1500 body diameters for high Mach number data and from about 500 body diameters for low Mach number data.

Electron Beam Experiment

The electron beam fluorescence probe has been successfully used in the study of gas densities in shock tubes and shock tunnels [29-31]. This technique has been selected to measure mass density in the wakes of hypersonic projectiles [32-33] because not only does this type of probe not mechanically interfere with the wake flow, but also it is capable of a good spatial and temporal resolution.

When a beam of electrons is fired through air or nitrogen, a small fraction of the electrons collide with the nitrogen molecules and excites them to radiative states. At gas densities low enough to prevent quenching effects, the fluorescence intensity is a linear function of gas density and electron beam current. As the fluorescent radiation is released almost instantaneously, the signal is proportional to the average gas density in any small volume from which the fluorescence is measured.

The excitation and emission processes involved have been analysed by Muntz [29] and the fluorescence of air and nitrogen have been studied spectrographically by O'Neil and Davidson [34]. The predominant radiation is emitted by the second positive system of the neutral nitrogen molecule N_2 (2+) and by the first negative system of the singly ionized nitrogen molecule N_2^+(1-). For test section pressures between 1.0 and 10 torr, the intensity of the N_2 (2+) system is more linear than for the N_2^+(1-) system. Also the linearity is better in pure nitrogen than in air as shown for the N_2 (2+) system in Figure 10. The 10 torr pressure limit is imposed not only by linearity considerations but also because, at higher pressures, the electron beam is strongly attenuated and

scattered.

The electron beam generator is capable of beam currents of 1 milliampere at accelerating potentials up to 100-kilovolts. Multiple pumping in the collimating section and the high accelerating potentials permit operation at test section pressures up to 10 torr. The light collecting and detecting system consists of a quartz lens and a slit defining a 1.2 by 12-mm field of view with the smaller dimension along the beam direction. A photograph of the range test section is shown in Figure 11. The electron beam collimating section is shown as it enters the range from the right. The electron beam is collected by the cup installed in the left side of the range. Three optical systems, each coupled with four detectors define fields of view at twelve radial positions with respect to the projectile flight line and along the electron beam axis.

Mass density measurements have been made in wakes of 2.7 inch diameter spheres fired at a velocity of 15,000 ft/sec in nitrogen atmospheres at a pressure of 7.6 torr. With a dispersion of shot at the measuring station of about one body diameter, the various firings gave density data at radial distances (R/D) which were slightly different for each firing. These data have been lumped together into six mean radial distances. The results are presented in Figure 12. Considering the centerline density (R/D = 0), there is first a low and constant density region extending approximately from X/D = 0 to X/D = 200 body diameters, associated with the laminar run of the wake. After this region, the wake experiences a large rate of density increase together with some rapid variations; these characteristics are associated with the turbulent flow regime. The radial distribution shows a continuous expansion as the axial distance increases. The density increase between X/D = 200 and 400 body diameters is attributed to the interference of the reflected bow shock. This reflected shock problem is aggravated at the electron beam station because of the large bulkhead supporting the electron gun which protrudes massively into the range for about 2 feet. The effect of the reflected shock is to produce a lateral displacement of the wake axis which appears as a density increase at 200 body diameters. When the bow shock reflected from the opposite side reaches the wake, it brings the wake back to its original position or nearly so; so the density decreases again at 400 body diameters. For firings of one inch diameter spheres in Range 5 the shock interference is felt only at 600 body diameters. Comparison with one inch sphere results indicates that the wake density results measured after the shock interference are valid. It should be pointed out that if the wake is assumed to be isobaric, it is possible to infer the wake temperature from the density data using the equation of state. Indeed inferred temperature curves similar to the density plots of Figure 12 are soon to be published[35].

Considerable data has recently been obtained with the electron beam equipment on both one inch and 2.7 inch sphere firings on Range 5, in the presence of the fiberglas wedge shock attenuation treatment. These data appeared to be considerably less affected by shocks and are in the process of being analyzed. The electron beam equipment is now being consecrated exclusively to cone wake studies.

Cooled-Film Anemometry

Hot wire anemometry has been applied to measurements of velocity and temperature characteristics of projectile wakes by Fox and his coworkers [18], at relatively low Mach numbers. In the hypersonic wake, the environmental temperature may exceed the operating temperature of conventional hot wires; in this case the cooled film anemometer developed by Fingerson[36] becomes attractive. The actual experimental technique in use at DREV is an application of the two-temperature method, where two anemometers are employed to determine both temperature and velocity. The analysis makes use of an empirical relation between Nusselt number and Reynolds number, such as that of Collis and Williams[37] to deduce both variables. A full description of these techniques has appeared in the literature[38].

Up to the present time, the technique has succeeded in providing measurements of the average temperature distribution in sphere wakes for distances behind the projectile exceeding 500 body diameters (Figure 13). Recent advances in the design of the electronic control system for the anemometer should permit improved measurements to be obtained in the wake of spheres starting immediately behind the body.

Electrostatic Probes and Microwave Scattering

Continuum electrostatic probes have been used at DREV since the beginning of the wake investigations. In axial arrays of 5 or more probes, they have succeeded in obtaining interesting velocity data[25] which was in excellent agreement with data obtained with the sequential spark technique (Figure 14), the two techniques confirming each other. Recent work with the electrostatic probes has again focussed on the original goal, the measurement of the statistical characteristics of the charge density fluctuations.

A large number of papers have been written about the theory of continuum electrostatic probes in a stationary plasma [39,40,41]. Examination of the more readily applicable of the various theories[42] indicates that ion current is functionally dependent on the product of temperature (raised to some power) and charge density (raised to some other power), where the electron, ion, and neutral temperatures have been assumed to be identical. Thus in the case of ion probes the theory indicates that the fluctuations observed in the current may be due to both ion density fluctuations and temperature fluctuations, with the result that correlations of probe current fluctuations will include influences of the autocorrelation of charge density, the autocorrelation of temperature, and the cross correlation of charge density and temperature fluctuations.

At low pressures the wake chemistry in the ballistic range is about frozen, so that one would expect the temperature fluctuations to be tightly

correlated with the electron density fluctuations. The space scales of the two fluctuating quantities should thus be very similar, and it appears reasonable to assume that the scales determined with the ion current observed under these conditions will in fact be the scales of the ion density fluctuations. At DREV signals obtained with electron and with ion collecting continuum probes appear to have the same statistical characteristics. This is fortunate because it does not appear that a useable theory for electron collection under continuum conditions is available. It is the electron density fluctuation statistics which are of interest for prediction of microwave scattering.

As the pressure increases in the wake, convection current (due to charge transported by the mean motion of a flowing ionized media) begins to become important relative to the mobility current. This introduces into the expression for the functional dependence of the probe current a factor which depends on flow velocity. Consequently fluctuations in flow velocity will produce fluctuations in probe current, and cross correlation terms involving velocity, temperature and charge density will contribute to the correlation function for the probe current. These conditions are to be avoided. At DREV the capability to fly a big sphere is important also in this regard, since it enables turbulent wakes to be studied under relatively low pressures.

Figure 15 represents probe currents obtained from a transverse array of five probes, each separated laterally by about 3/8 inch (or approximately 0.15 body diameters). Two of the probes were parallel to the wake flow and three were perpendicular to the flow. Despite a difference of a factor of 10 in presented area to the mean flow direction, all the probes collected about the same current, allowing for natural variation of the charge density distribution with radial distance. In other words, the probe current was not significantly affected by wake velocity effects,and thus it can be safely assumed that the probe currents are dependent only on the scalar qualities of temperature and charge density. Using the knowledge of the temperature distribution across the wake obtained through the electron beam experiment and integrated measurements of the electron density through the wake obtained with a microwave interferometer bridge, an attempt will be made at DREV to deduce the exponents of temperature and electron density in the expressions for the functional dependence of probe current.

In addition to continuum electrostatic probe experiments, an attempt is underway to operate a Langmuir probe experiment in Range 5, following the suggestion of Sutton(43). This is a delicate experiment because of the necessity of using very fine wires to minimize continuum flow effects, and because of the difficulty of ensuring probe cleanliness.

Associated with the electrostatic probe measurements of fluctuating charge densities, and the interferometer measurements of mean electron density, DREV is operating an X-band microwave scattering experiment. The basic configuration of the experiment has the transmitter antenna and six receiving horns located around the interior of the range diameter; all horns are oriented in the same plane perpendicular to the line of flight, with the electric field vector parallel to the flight path. Linear polarization of the dominant TE_{10} mode is maintained at the horn-lens antenna unit, with essentially far field conditions for the antennae applying at the center of the range. All horns see exactly the same scattering volume. Defining 180° as the back scatter angle with respect to the transmitter, the receiver heads are situated at 150°, 135°, 105°, 90°, 75°and 45° (Figure 16).

Results obtained with the scattering experiment are promising. Figure 17 shows signals recorded from the six receiver channels on a sphere firing in nitrogen at 7.6 torr. Estimates of the scattered power distribution as a function of scattering angle for a number of 20 torr and 7.6 torr air and nitrogen rounds were normalized at a scattering angle of 150°, and plotted against the Booker-Gordon theory prediction for an exponential behavior of the electron density fluctuation correlation function. The initial comparison (Figure 18) is not unreasonable.

IV. CONCLUSIONS

Since 1965, significant progress and accomplishments have been achieved in the field of spatially-resolved or point measurements of various aerothermochemical parameters in the turbulent wakes of hypersonic projectiles. The sequential spark technique for velocity measurement has been applied to sphere wakes with outstanding success and data has been collected or is being collected over a range of axial distance extending from about 10 body diameters to several thousand. The electron beam technique has been used to obtain mass density distributions across sphere wakes over essentially the same range of axial distance and the data has been inverted to infer temperature distributions throughout the wake. Electrostatic probes have also been used in axial pairs to measure sphere wake convection velocities and the data have been found to be in excellent agreement with sequential spark data. Renewed confidence exists that probe measurements interpretable in terms of charge density and charge density fluctuations can be made in the hypersonic wake and the fluctuating density space scales obtained have been of some use in predicting the angular dependence of microwave power scattered from the wake as subsequently observed with the angular diversity scattering experiment. A cooled film anemometer two-temperature technique has apparently overcome a series of development problems, and, having given reasonable measurements of wake temperature beyond about 500 body diameters behind a projectile, now appears likely to be capable of mapping the complete temperature wake, starting from the projectile.

A list of minimum objectives for the remainder of the DREV-ARPA program would be as follows: First of all, a series of data rounds are required with the cooled film anemometer. Similarly a series of data rounds with the survey

arrays of continuum electrostatic probes must be analyzed, and the characteristic comportment of probe current as a function of charge density firmly established. These results should be compared with the results of measurements with Langmuir type electrostatic probes. While the feasibility of the Langmuir probe measurements are not completely established, it is possible that absolute measurements of electron density will be possible with this device. Finally both the sequential spark technique and the electron beam will be applied to the measurement of velocity and mass density profiles in cone wakes.

ACKNOWLEDGEMENTS

This work was partially sponsored by the Advanced Research Projects Agency under contract DAAH01-69-C-0921.

This paper is a summary of the work of many contributors namely Dr. D. Heckman on reflected shocks, electrostatic probes and microwave scattering, Mr. D. Ellington on cooled film anemometry, Messrs J.G.G. Dionne and L.Tardif on the electron beam experiment and Mr. C. Lahaye on the sequential spark experiment. The author is indebted to all these scientists and in particular to Dr. D. Heckman for having collated the material. The members of the Aero-Systems Engineering Section under Mr. P. Solnoky and Range Instrumentation Section under Dr. E.G. Léger have also contributed in an important manner over the years to the obtaining of these results and their efforts are here acknowledged.

REFERENCES

1. Bull, G.V., "Re-entry Studies in Free Flight Ranges." Proceedings of the Seventh Anglo-American Aeronautical Conference, pp. 312-343, published by the Institute of the Aeronautical Sciences, New York, N.Y., 1959.

2. Wilenius, G., M. Cloutier and P.L. Cowan, "Theoretical Analysis of a Constant Base Pressure Light Gas Gun," CARDE TM/703/62, October/62.

3. Cloutier, M., "An Experimental and Theoretical Study of the CARDE 4-inch Light Gas Gun," CARDE TN/1772/66, June 1966.

4. Primich, R.I., "Microwave Techniques for Hypersonic Ranges," Paper in "Electromagnetic Effects of Re-Entry," Pergamon Press, pp. 186 (1961).

5. St. Pierre, C., "Emitted Radiation Studies Performed in a Hypersonic Range with 1/2-In. Models," CARDE TM AB-52.

6. Kornegay, W., "Electron Density Decay in Wakes", AIAA Journal, 3, p. 1819 (1965).

7. Hayami, R.A., and Primich, R.I., "Wake Electron Density Measurements behind Hypersonic Spheres and Cones," Proceedings of the AGARD Specialists Meeting on Fluid Physics of Hypersonic Wakes, held at Colorado State University, Fort Collins, Colorado, 10-12 May 1967.

8. Slattery, R.E. and W.G. Clay, "Width of the Turbulent Trail behind a Hypervelocity Sphere," Phys. Fluids 4, 1199, (1961).

9. Herrmann, J., R.E. Slattery and W.G. Clay, "Measured Properties of the Wakes of Hypersonic Cones." AIAA Fluid and Plasmas Dynamics Conference, June 1968, AIAA Paper No. 68-687.

10. Pippert, G.F., "On the Structure of Wake Turbulence Deduced from Field Radar Measurements," AIAA Preprint 63-446 (1963).

11. Menkes, J., "Scattering of Radar Waves by an Underdense Turbulent Plasma," AIAA Journal, Vol. 2, No.6, 1154-56, June, 1964.

12. Zeiberg, S.L. and G.D. Bleich,"Finite-Difference Calculation of Hypersonic Wakes," AIAA Vol. 2, pp. 1396-1402, August 1964.

13. Lykoudis, Paul S., "A Review of Hypersonic Wake Studies." AIAA Journal, Vol. 4, No. 4, April 1966, p. 577.

14. Solnoky, P., "Free Flight Simulation from Mach 1 to Mach 30 in the Hypersonic Range." Canadian Aeronautics and Space Journal, Vol. 15, No. 9, November 1969.

15. Normand, M., "A Review of Model Design for Free Flight Aerodynamic Studies," CARDE T.N. 1657/65, February 1965.

16. Heckman, D.L. Tardif, and C. Lahaye, Experimental Study of Turbulent Wakes in the CARDE Free-Flight Ranges," Proceedings of the Symposium on Turbulence of Fluids and Plasmas, published by the Polytechnic Press, of the Polytechnic Institute of Brooklyn, 1969.

17. Knystautas, R., "The Growth of the Turbulent Inner Wake Behind a Three-Inch Diameter Sphere," TR 488, Jan. 1964, CARDE.

18. Fox, J., et al., "Hot-Wire Measurements of Wake Turbulence in a Ballistic Range." AIAA Journal, Vol. 5, No. 1, pp. 99-104, January 1967.

19. Kornegay, W.M., "Resonant Cavity Measurements of Ionized Wakes," IEEE Trans., Vol AES-4, No. 2, pp. 181-186, March, 1968.

20. Heckman, D., C. Lahaye, L. Moir, B. Podesto and W. Robertson," A Shock Wave Attenuation Treatment for Ballistic Ranges," Accepted for publication in the AIAA Journal.

21. Robertson, W.J., "The Effect of Reflected Shock Systems on Hypersonic Wakes," DREV T.N. 1846/69, October 1969.

22. Pao, S.P., "Shock Reflection Elimination System for the CARDE Hypersonic Ballistic Range Facility," Wyle Laboratories - Research Staff Consulting Report No. WCR 69-2, June 1969.

23. Bomelburg, H.J., J. Herzog, and J.R. Weske, "The Electric Spark Method for Quantitative Measurements in Flowing Gases." AFOSR TN-59-273, ASTIA AD212707, University of Maryland

(1959), Unclassified.

24. Frungel, F.B.A., High Speed Pulse Technology" (New York: Academic Press 1956) pp. 162-182.

25. Heckman, D, A. Cantin, A. Emond and A. Kirkpatrick, "Convection Velocity Measurements in Hypersonic Spheres Wakes." AIAA Journal 6, 4, pp.750-52, April 1968.

26. Fox, J., and H. Rungaldier, "Anemometer Measurements of Velocity and Density in Projectile Wakes." AIAA Fluid and Plasma Dynamics Conference, June 1968, AIAA Paper No. 68-701.

27. Lahaye, C., E.G. Leger, and A. Lemay, "Wake Velocity Measurements using a Sequence of Sparks." AIAA J. Vol. 5, No. 12, pp. 2274-2276, December 1967.

28. Lahaye, C., E.G. Leger and A. Lemay, "Radial and Axial Velocity Profiles of Hypersonic and Supersonic Wakes Measured by the Sequential Spark Method." AGARD Conference Proceedings No. 19, Fluid Physics of Hypersonic Wakes Conference, May 1967.

29. Muntz, E.P., "Static Temperature Measurements in a Flowing Gas," The Physics of Fluids, Vol 5, No. 1, Jan 1962, pp. 80-90.

30. Muntz, E.P. and Softley, E.S., "A Study of Laminar Near Wakes." AIAA Journal Vol.4, No. 6, June 1966, pp. 961-968.

31. Rothe, D.E., "Electron Beam Studies of the Diffusive Separation of Helium-Argon Mixtures." The Physics of Fluids, Vol.9, No.9 Sept 1966, pp. 1643-1658.

32. Dionne, J.G.G., Sadowski, C.M., Tardif, L., and Vanoverschelde, J.E.H., "Mass Density Measurements in Hypersonic Wakes." AGARD Conference Proceedings No.19, Fluid of Physics of Hypersonic Wakes, Colorado State University, May 1967.

33. Tardif, L., and Dionne, J.G.G., "Density Distribution in Turbulent and Laminar Wakes." AIAA Journal, Vol. 6, No. 10, October 1968, pp. 2027-2029.

34. Davidson, G. and O'Neill, R., "The Fluorescence of Air and Nitrogen Excited by 50 Kev Electrons." AFCRL-64-466, May 1964, Air Force Cambridge Research Lab, Bedford, Mass.

35. Dionne, J.G.G. and Tardif, L. "Mean Density and Temperature Data in Wakes of Hypersonic Spheres." Submitted to the AIAA Journal.

36. Fingerson, L., "Instruction Manual,Heat Flux System Model 1000A," (St. Paul, Minn: Thermosystems Inc.).

37. Collis, D.C., and William, M.H. "Two Dimensional Convections from Heated Wires at Low Reynolds Numbers," J. Fluid Mech 6, 3, pp. 357-384 (October 1959).

38. Ellington, D. and Trottier, G., "Studies of Turbulence in the Wakes of Hypersonic Spheres under Simulated Reentry Conditions," Proceedings of the AGARD Specialists Meeting on Fluid Physics of Hypersonic Wakes, held at Colorado State University, Fort Collins, Colorado, 10-12 May 1967.

39. Shulz, G.J., and Brown, S.C., "Microwave Study of Positive Ion Collection by Probes," Phys. Rev., Vol. 98, No. 6, 1642-1649, June 15, 1955.

40. Zakharova, V.M., Kagan, Yu.M., Mustafin, K.S., and Perel, V.I. "Probe Measurements at Medium Pressures," Zh. Techn. Fiz. 30, 411, 1960 (English Translation: Soviet Physics - Tech. Phys. Vol. 5, 411-417, 1960).

41. Su, C.H., and Kiel, R.E., "Continuum Theory of Electrostatic Probes," Jour. Applied Physics, Vol. 37. No. 13, 4907-10, December 1966.

42. Cantin, A., A. Emond, D. Heckman, "Observations on Electrostatic Probe Behavior in Collision-Dominated Ionized Turbulent Gas Flows in Ballistic Ranges," ICIASF'69 Record, published by IEEE Transactions on Aerospace and Electronic Systems, May 1969.

43. Sutton, G.W., "Use of Langmuir Probes for Hypersonic Turbulent Wakes." AIAA Journal, Volume 7, No. 2, p. 193, February 1969.

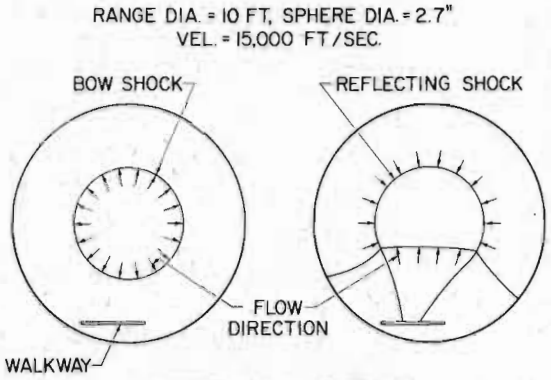

OUTGOING & REFLECTING SHOCK SYSTEM IN ASYMMETRIC RANGE 5 GEOMETRY

FIGURE 1: The presence of the walkway in Range 5 produces an asymmetry in the reflected shock system.

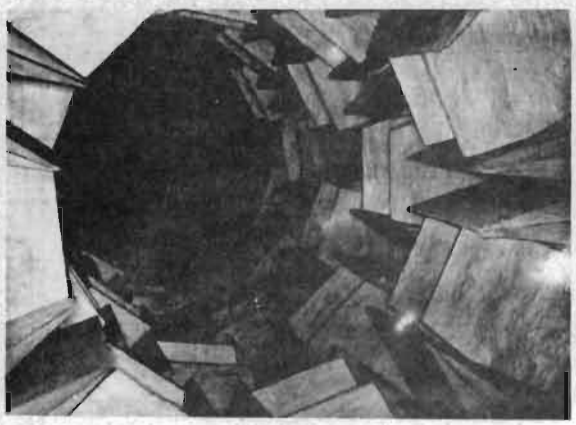

FIGURE 2: Anechoic fiberglas wedge treatment installed in a small cylinder for evaluation. The planes of symmetry through the individual wedges were approximately normal to the imparting shock wave.

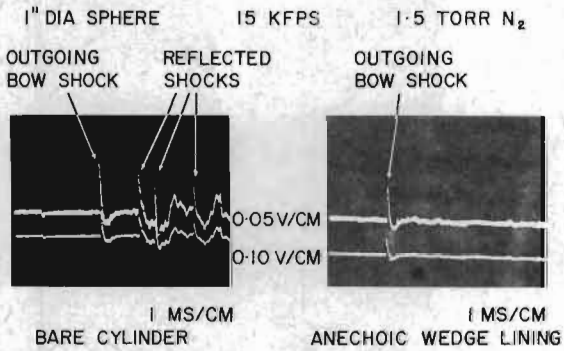

FIGURE 3: Pressure transducer measurements in the anechoic wedge treatment compared to results in a bare cylinder. The reflected shocks are not detected in the treated cylinder.

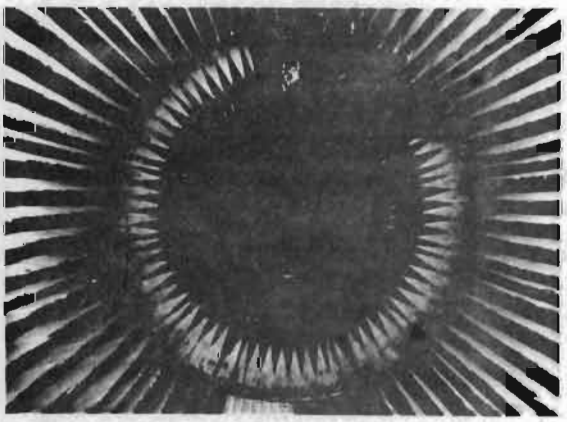

FIGURE 4: Shock wave attenuation treatment installed in the interior of hypersonic range facility No. 5. The photograph shows a section of the carriage which rolls over the walkway to complete the treatment.

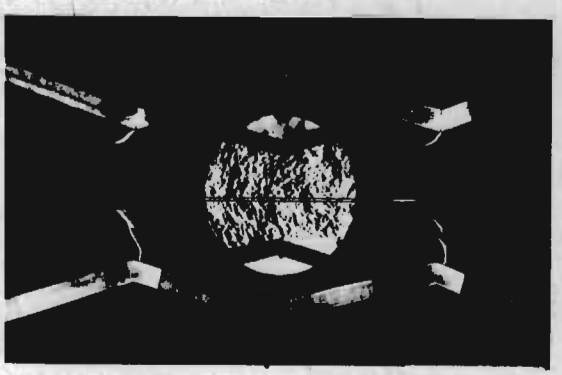

FIGURE 5: Stereo-photographs of a sequence of sparks together with a Schlieren photograph of the wake.
X/D = 600; V_∞ = 14.6 kfps; P_∞ = 40 torr.

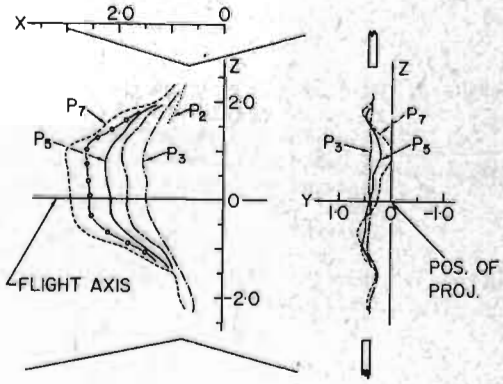

FIGURE 6: Projections in the XZ (axial) and YZ (lateral) plane of the series of sparks of Figure 5.

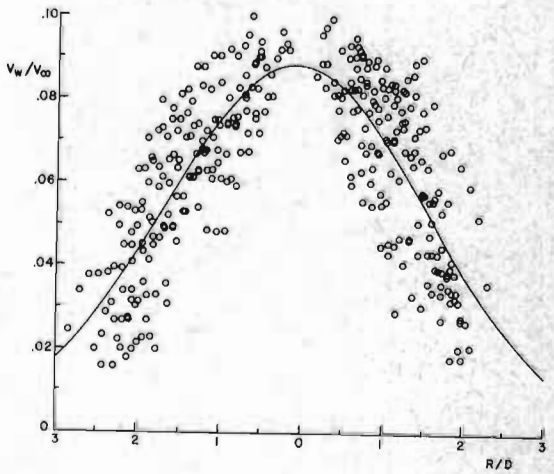

FIGURE 7: Typical set of data from 12 measurements at 300 body diameters behind one inch diameter spheres (V_∞ = 14500 fps; P_∞ = 40 torr). The wake axial velocity (Vw) is normalized to the sphere velocity (V_∞) and the radial distance (R) to the sphere diameter (D). Also shown is the slightly asymmetric Gaussian curve fitted to the data.

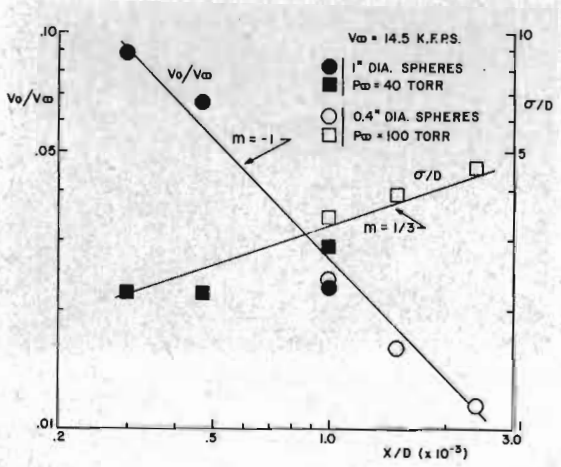

FIGURE 8: Wake axis velocities (Vo/V_∞) and velocity profile widths (σ/D) determined from least mean square fits of Gaussian curves to sets of data measured at various axial distances (X/D). Full lines represent power laws with slopes of -1 and 1/3 fitted to the wake axis velocity and the velocity profile width data respectively.

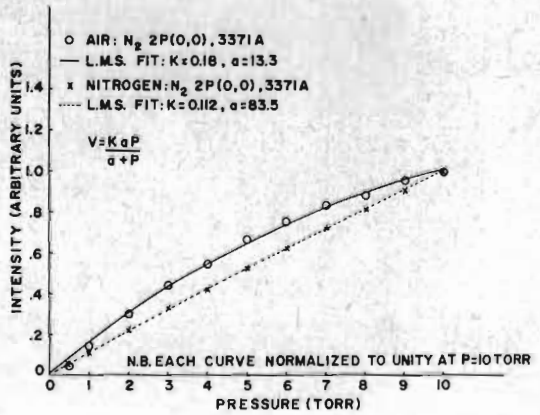

FIGURE 10: Fluorescence intensity as a function of gas pressure.

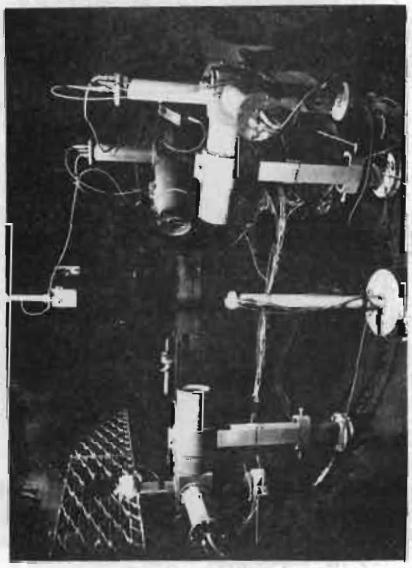

FIGURE 11: Electron beam installation in ballistic range.

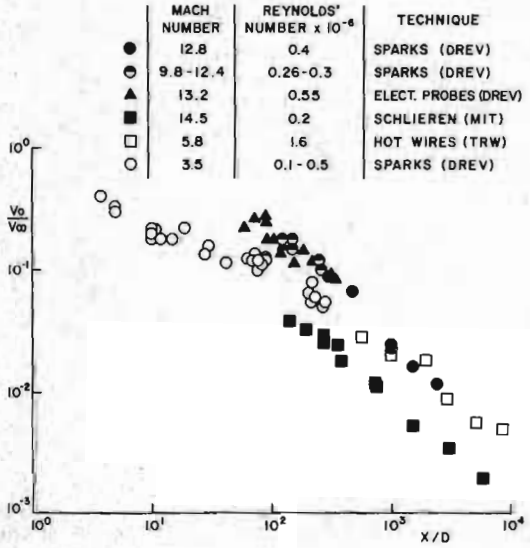

FIGURE 9: Comparison of sphere wake velocities measured in ballistic ranges by four different experiments: sequential spark, electrostatic probe, hot wire and sequential schlieren techniques.

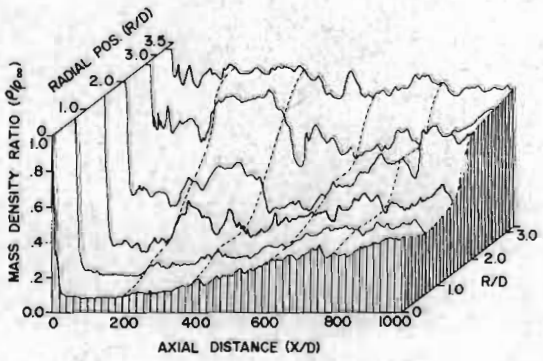

FIGURE 12: Mass density distribution in a turbulent wake of a 2.7 inch diameter Titanium sphere (P_∞ = 7.6 torr N_2 and V_∞ = 15,000 ft/sec.)

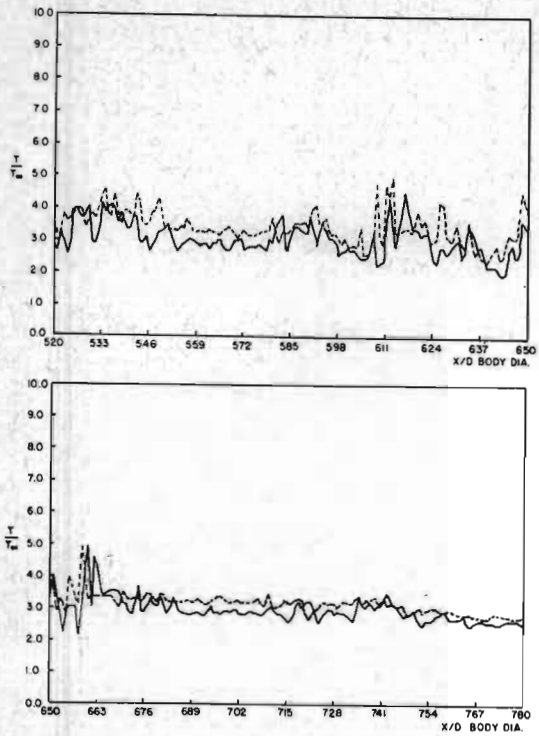

FIGURE 13: Temperature data obtained with two pairs of cooled film anemometers using the two-temperature method to deduce temperature and velocity. The two pairs of probes were interleaved so as to see as nearly as possible the same wake environment. The projectile was a 2.7 inch diameter sphere, and the radial distance of the probes from the wake axis was 1.46 body diameters (V_∞ = 15,000 ft/sec, P_∞ = 76 torr).

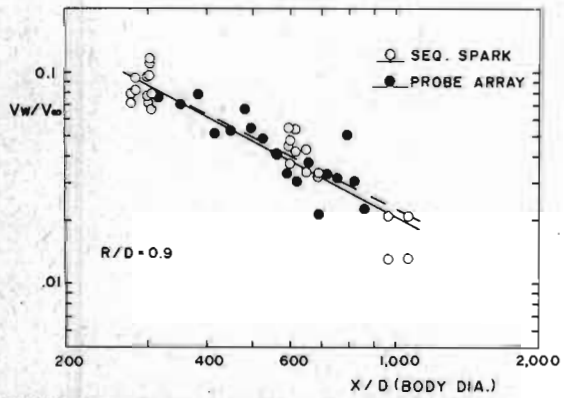

FIGURE 14: Power law fits of sequential spark and electrostatic probe array velocity data at R/D = 0.9. The spark data is from one inch diameter sphere firings at 40 torr and velocities from 12,000 to 15,000 ft/sec, while the probe data is from 2.7 inch sphere firings at 20 torr and velocities from 14,000 to 15,000 ft/sec.

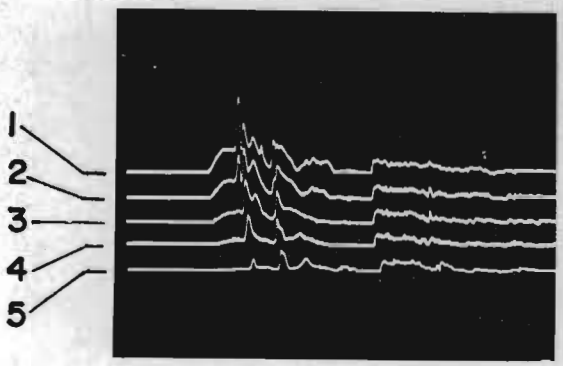

FIGURE 15: Probe current from ion probes in the turbulent wake of a hypersonic sphere at low pressure. Probes 1, 3, and 5 were oriented perpendicularly to the mean wake flow while probes 2 and 4 were parallel to the flow. The conclusion from these results is that there is no significant convected component in the probe current.

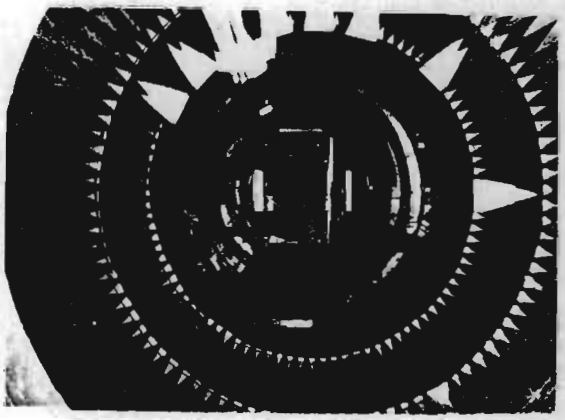

FIGURE 16: Geometry of microwave scattering experiment in Range 5. The transmitter is located at three o'clock on the right hand side of the range. Moving counterclockwise, receivers are located at 135°, 105°, 90°, 75°, 45° and 30°.

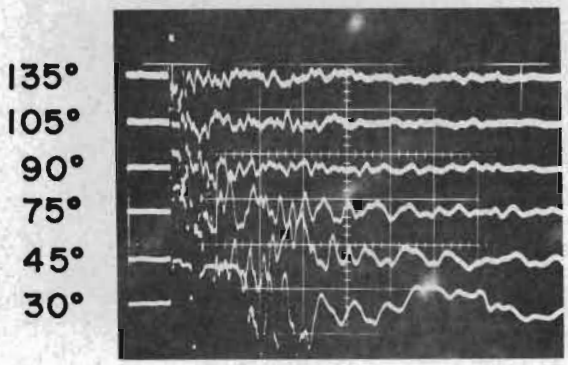

FIGURE 17: Typical microwave scattering signals from the turbulent wake of a 2.7 inch diameter sphere in Range 5.

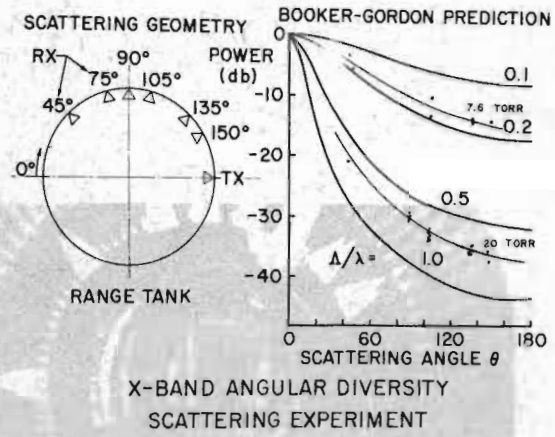

FIGURE 18: Comparison of some preliminary scattered power results from the microwave scattering experiment with the predictions of the Booker-Gordon theory.